Violet-to-Blue Tunable Emission of Aryl-Substituted Dispirofluorene-Indenofluorene Isomers by Conformationally-Controllable Intramolecular Excimer Formation

ARTICLE *in* CHEMISTRY - A EUROPEAN JOURNAL · SEPTEMBER 2011

Impact Factor: 5.73 · DOI: 10.1002/chem.201100971 · Source: PubMed

6 AUTHORS, INCLUDING:

Cyril Poriel
Université de Rennes 1
73 PUBLICATIONS **1,005** CITATIONS
SEE PROFILE

Joëlle Rault-Berthelot
Université de Rennes 1
106 PUBLICATIONS **1,707** CITATIONS
SEE PROFILE

CHEMISTRY
A EUROPEAN JOURNAL

DOI: 10.1002/chem.201100971

Violet-to-Blue Tunable Emission of Aryl-Substituted Dispirofluorene–Indenofluorene Isomers by Conformationally-Controllable Intramolecular Excimer Formation

Damien Thirion,[a] Cyril Poriel,*[a] Rémi Métivier,[b] Joëlle Rault-Berthelot,[a] Frédéric Barrière,[a] and Olivier Jeannin[a]

Abstract: Two series of DiSpiroFluorene–IndenoFluorene (DSF-IF) positional isomers, namely dispiro[2,7-diarylfluorene-9′,6,9″,12-indeno[1,2-*b*]fluorenes], (1,2-*b*)-DSF-IFs **1** and dispiro[2,7-diarylfluorene-9′,6,9″,12-indeno[2,1-*a*]fluorenes], (2,1-*a*)-DSF-IFs **2** have been synthesized. These violet-to-blue fluorescent emitters possess a 3π-2spiro architecture, which combines via two spiro links two different indenofluorene cores, that is, (1,2-*b*)-IF or (2,1-*a*)-IF and 2,7-substituted-diaryl-fluorene units. Due to their different geometric profiles, the two families of positional isomers present drastically different properties. The marked difference observed between the properties of (1,2-*b*)-DSF-IF (**1**) and (2,1-*a*)-DSF-IF (**2**) is discussed in terms of intramolecular π–π interactions occurring in (2,1-*a*)-DSF-IF (**2**) leading to conformationally-controllable intramolecular excimer formation. Indeed, the original geometry of the (2,1-*a*)-DSF-IF (**2**) family, with face-to-face "aryl-fluorene-aryl" moieties, leads to remarkable excimer emission through intramolecular π–π interactions in the excited state. Furthermore, the emission wavelengths can be gradually modulated by the control of the steric hindrance between the adjacent substituted phenyl rings. Thus, through a comparative and detailed study of the ^{1}H NMR, electrochemical and photophysical properties of DSF-IFs **1** and **2**, we have evidenced the intramolecular π–π interactions occurring between the two "aryl-fluorene-aryl" moieties in the ground state and in the excited state. These properties have been finally correlated to the spectacular conformational change modeled by density functional theory (DFT) calculations. Indeed, the two "aryl-fluorene-aryl" moieties switch from a staggered conformation in the ground state to an eclipsed conformation in the first excited state.

Keywords: fluorescence · excimer · indenofluorene · intramolecular π–π interactions · spiro compounds

Introduction

For the last two decades of research in organic electronics, significant efforts have been devoted to the design and the synthesis of original π-conjugated molecules with specific properties.[1–5] As the photophysical properties of organic molecules are influenced by π–π interactions,[6] the synthesis, via a common intermediate, of different molecules possessing distinct geometry profiles that allow or not intramolecular π–π interactions constitutes an appealing strategy for tuning the properties of organic materials. For example, in fluorescent molecules, π–π interactions may cause a red-shift of the emission wavelength by excimer formation.[6] Indeed, excimer formation resulting from intramolecular interactions have been widely described in the literature for various systems such as naphthalene,[6] oligophenyl based cruciforms,[7] ethynyltriphenylene derivatives,[8] dibenzofulvene polymers with fluorene side chains,[9] carbazolophanes[10] and stilbenophanes,[11] and various pyrene[6,12–14] and thiophene derivatives.[15–18] Despite their importance in the field of organic light emitting diodes (OLED),[3–5,19–23] intramolecular excimer fluorescence of "aryl-fluorene-aryl" derivatives have only been very recently investigated.[24] Our group has indeed reported preliminary results on the marked difference observed between two families of positional isomers, namely (1,2-*b*)-DSF(R)$_4$-IF **1** and (2,1-*a*)-DSF(R)$_4$-IF **2**.[24] These molecules, synthesized via a common intermediate, present distinct geometry profiles that translate into drastically different optical properties leading for (2,1-*a*)-DSF(R)$_4$-IFs **2** to conformationally-controllable intramolecular excimer formation. In this paper,

[a] D. Thirion, Dr. C. Poriel, Dr. J. Rault-Berthelot, Dr. F. Barrière, Dr. O. Jeannin
Université de Rennes 1, UMR CNRS 6226
"Sciences Chimiques de Rennes", Bat 10C, Campus de Beaulieu
35042 Rennes cedex (France)
Fax: (+33) 223-236732
E-mail: cyril.poriel@univ-rennes1.fr

[b] Dr. R. Métivier
PPSM, ENS Cachan, CNRS, UniverSud, 61 av President Wilson
94230 Cachan (France)

Supporting information for this article is available on the WWW under http://dx.doi.org/10.1002/chem.201100971: Materials and methods, full experimental procedures and spectroscopic characterization and copy of ^{1}H and ^{13}C NMR spectra for all new compounds, CV, DPV, TGA, fluorescence decay and 2D NMR spectra of all IF and DSF-IFs, X-ray structures of **2c** and **2e**.

we report a detailed investigation of intramolecular π–π interactions occurring between the two face-to-face "aryl-fluorene-aryl" moieties of (2,1-*a*)-DSF(R)$_4$-IFs **2** in the ground state and in the excited state. First, through a comparative and detailed study of the ^{1}H NMR, electrochemical and absorption properties of type **1** and **2** molecules, we look for possible π–π interactions in the ground state. Then, fluorescence experiments are analyzed, in particular in terms of intramolecular excimer formation in the excited state of type **2** molecules. Finally, the spectacular excimer effect in **2** is shown to be finely tuned with the steric bulk borne by the phenyl groups of the fluorene moieties. DFT modeling of these properties suggest a conformational switch of the two "aryl-fluorene-aryl" moieties from a staggered conformation in the ground state to an eclipsed conformation in the first excited state.

Results and Discussion

Synthesis

DSF-IFs **1** and **2** were synthesized according to our previously published synthetic pathway (Scheme 1).[24–26][1] The aryl-substituted fluorenones **3c–g** were prepared through an efficient two-step synthesis (Scheme 1). In this sequence, 9-fluorenone was first iodinated in the presence of *N*-iodosuccinimide in acidic medium to afford **5** with 83% yield.[27,28] Oppositely to the widely-used analogue 2,7-dibromo-fluorenone, 2,7-diiodofluorenone **5** is highly soluble in common organic solvents and thus appears to be an interesting and easy to handle intermediate in fluorene chemistry. The Suzuki–Miyaura palladium-catalyzed cross-coupling reaction[29] of **5** with aryl-substituted boronic acids led to the corresponding fluorenones **3c–g** with high yields. Then, the lithium-iodine exchange of 2,2″-DITP[26] with *n*-butyllithium followed by addition of **3c–g** afforded the corresponding difluorenol **4c–g** with moderate yields (22–44%). The intramolecular cyclization reaction of **4c–g**, performed in the presence of either a Lewis (trifluoride boron etherate) or a Brönsted acid (H_2SO_4, HCl) leads to the formation of two positional isomers (1,2-*b*)-DSF-IFs **1** and (2,1-*a*)-DSF-IFs **2**, further separated by column chromatography. It is important to note that the ratio of DSF-IFs **1** and **2** obtained by the cyclization of the diols **4** may be tuned by solvent and steric effects as previously reported.[30] The chemical structures and the purity of the molecules investigated in the present work have been confirmed by means of ^{1}H NMR, ^{13}C NMR, IR spectroscopy and mass analysis. X-ray structures of **2c** and **2e** are presented in the Supporting Information (Figures S1 and S2).

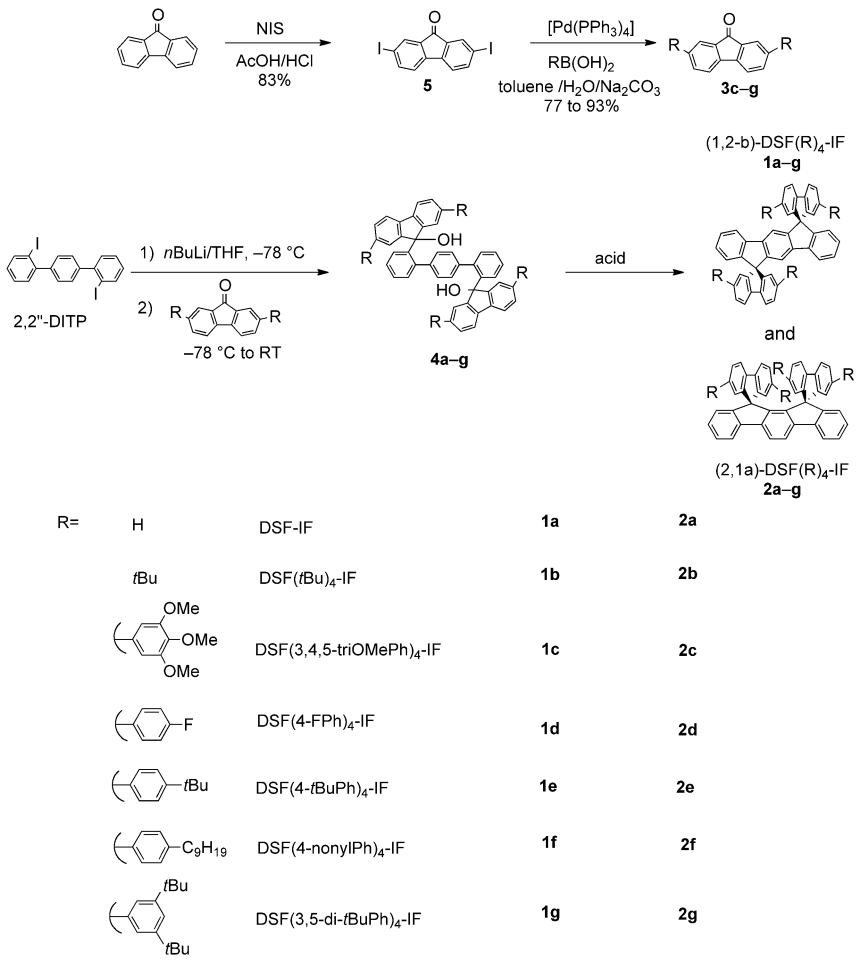

Scheme 1. Synthesis of aryl-substituted 9-fluorenone **3c–g** and DSF-IFs **1a–g**/**2a–g**.

For the intimate understanding of the spectroscopic properties of DSF-IFs **1** and **2**, it was of great interest to compare them to those of their constituting building blocks (Scheme 2). For that, different model systems were investigated: The two parent indenofluorenes, (1,2-*b*)-IF[26] and (2,1-*a*)-IF,[31] 9,9′-spirobifluorene (SBF),[4] and 2,7-di(4-nonylphenyl)-9,9′-spirobifluorene (**m1**, see Supporting Information) model compound for the isomers **1f**/**2f**.

^{1}H NMR spectroscopy studies

A detailed ^{1}H NMR characterization of all DSF-IFs **1** and **2** has been first performed in order to correlate the different

[1] The synthesis of 9-fluorenone **3b** has been previously reported.[25]

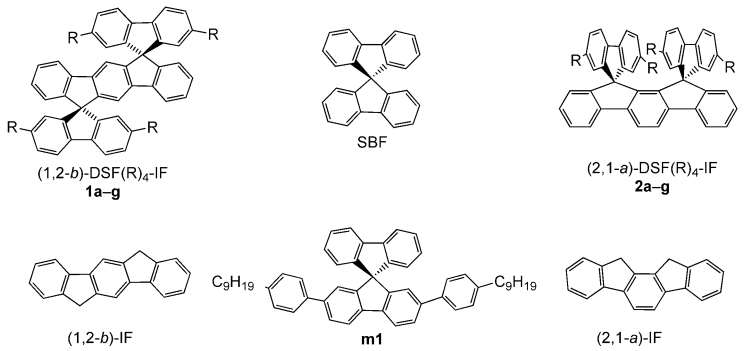

Scheme 2. Structure of DSF-IF, SBF and IF derivatives and the model compound **m1**.

chemical shifts of the hydrogen atoms to the molecular structures of the two DSF-IFs families (see Tables S1–S3 in the Supporting Information). The purpose of these detailed and comparative ^{1}H NMR investigations is to determine if intramolecular π–π interactions could occur in solution between "aryl-fluorene-aryl" moieties in the DSF-IFs **2**. In assigning ^{1}H NMR spectra of molecules **1** and **2**, the following numbering is used, in which H1–H4 belong to the fluorene moieties, H5–H9 belong to the indenofluorene core and H10–H12 belong to the pendant aryl rings of the fluorenyl units (Figure 1). The complete assignments of all molecules

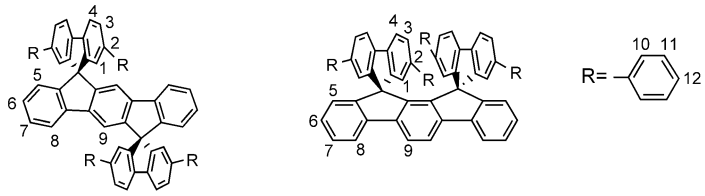

Figure 1. Numbering used for the ^{1}H NMR assignments.

have been performed by 2D NMR spectroscopy experiments (see Supporting Information for spectra and tables).

^{1}H NMR chemical shifts of the indenofluorene core: We first report on the two parent indenofluorene derivatives, that is, (1,2-*b*)-IF and (2,1-*a*)-IF (Scheme 2) respectively central core of the DSF-IF type **1** compounds and of the DSF-IF type **2** compounds. In (1,2-*b*)-IF and (2,1-*a*)-IF, all the hydrogen atoms possess almost identical chemical shifts (Table S1 in the Supporting Information). Only a slight difference is observed for the H9 resonance (δ = 7.97 ppm for (1,2-*b*)-IF and δ = 7.83 ppm for (2,1-*a*)-IF). Hence, the isomers (1,2-*b*)-IF and (2,1-*a*)-IF present highly similar ^{1}H NMR spectra due to their comparable molecular structure. However, DSF-IFs **1** and **2**, exhibit a significantly different behavior as their ^{1}H NMR spectra appear to be fairly different. In the following study, we will first compare the ^{1}H NMR spectra of the DSF-IFs **1** and **2** with their respective central cores, namely (1,2-*b*)-IF and (2,1-*a*)-IF. In a second step, the ^{1}H NMR spectra of DSF-IFs **1** and **2** will be compared to one another.

Compared to the parent indenofluorene (1,2-*b*)-IF, all the DSF-IFs **1** present a strong shielding effect for signals of the two hydrogen atoms in β position of the spiro carbons, namely H5 and H9. Indeed, the resonance of H5 is found at δ 7.57 ppm in (1,2-*b*)-IF and at about 6.7 ppm in all the DSF-IFs **1** (Table S1). Similarly, the resonance of H9 is found at 7.97 ppm in (1,2-*b*)-IF and at about 7.2 ppm in all DSF-IFs **1** (Table S1). This upfield shift found for H5 and H9 resonances, in all DSF-IFs **1**, is due to the different substitution of the bridges (CH_2 for (1,2-*b*)-IF and fluorene units for DSF-IFs **1**). This shielding effect, also observed for H6, H7 and H8 resonances, decreases from H5 to H8 as the distance from the spiro centers increases. In addition, **1a–b**, without aryl rings on the fluorene units, and **1c–g**, bearing aryl rings on the fluorene units, present highly similar chemical shifts for all the hydrogen atoms of the (1,2-*b*)-indenofluorenyl moiety (Table S1). Hence, the 2,7-substitution of the fluorene units with aryl rings, found in **1c–g**, has only a minor effect on the chemical shifts of the hydrogen atoms of the (1,2-*b*)-indenofluorenyl core.

Compared with the parent indenofluorene (2,1-*a*)-IF, all the DSF-IFs **2** also present a strong shielding effect for the hydrogen atom H5 resonance from δ 7.60 ppm in (2,1-*a*)-IF to about 6.1 ppm in all the DSF-IFs **2** (Table S1). This shielding effect, arising from the spirolinked fluorene units, is even larger than that observed between (1,2-*b*)-IF and the DSF-IFs **1** (see above). This shielding effect highlights that the fluorene units in DSF-IFs **1** or in DSF-IFs **2** have drastically different electronic effects on their corresponding indenofluorenyl central cores. As already highlighted above for **1c–g**, the 2,7-substitution of the fluorene moieties with aryl rings has only a weak influence on the chemical shifts of the hydrogen atoms of the (2,1-*a*)-indenofluorenyl core. Therefore all the DSF-IFs **2** with or without aryl rings present highly similar ^{1}H NMR chemical shifts for their central indenofluorenyl core.

An important feature is related to the differences observed between the chemical shifts of the hydrogen atoms of the indenofluorenyl cores of the two DSF-IF families. Thus, in DSF-IFs **2**, H5 and H6 signals are surprisingly shielded by 0.6/0.7 ppm and by 0.1/0.2 ppm compared with their homologues in DSF-IFs **1**, whereas the two parent indenofluorenes, that is, (2,1-*a*)-IF and (1,2-*b*)-IF present almost identical chemical shifts for all their hydrogen atoms (Table S1). This surprising shielding effect observed between DSF-IFs **2** and DSF-IFs **1**, has been assigned to their different geometry profiles. Indeed, in DSF-IFs **2**, the (2,1-*a*)-indenofluorenyl core is influenced by the two face-to-face spirofluorene units, which may interact together (see below). Oppositely, in DSF-IFs **1**, the (1,2-*b*)-indenofluorenyl core is influenced by only one fluorene unit as the fluorene units are on two opposite sides of the indenofluorenyl core.

In summary, (1,2-*b*)-IF and (2,1-*a*)-IF, present almost identical chemical shifts for all the hydrogen atoms, whereas the

hydrogen atoms of the indenofluorenyl cores of DSF-IFs **1** and **2** were found at very different chemical shifts. Thus, the different arrangement of the fluorene units (face-to-face or not) differently affects the resonance of the hydrogen atoms of the indenofluorenyl cores.

^{1}H NMR chemical shifts of the spiro-linked fluorene units: The distinct geometries of DSF-IFs **1** and **2** should lead to significant chemical shift differences of the hydrogen atoms of the fluorene moieties. In order to study the possible interactions between the two face-to-face fluorene units in DSF-IFs **2**, the ^{1}H NMR investigations were first conducted on the simplest analogues in the series, **1a–b**, **2a–b** without pendant aryl rings, and compared with a relevant model compound, namely 9,9′-spirobifluorene (SBF, see structure Scheme 2).

The fluorene units of **1a** and SBF present hydrogen atoms with almost identical chemical shifts (Table S2 in the Supporting Information), clearly highlighting that the fluorene units of both molecules are in a very similar chemical environment. For **2a**, an upfield shift of about 0.3/0.7 ppm is detected for all the signals of the hydrogen atoms borne by the fluorene units (Table S2, Figure 2, bottom). This shielding

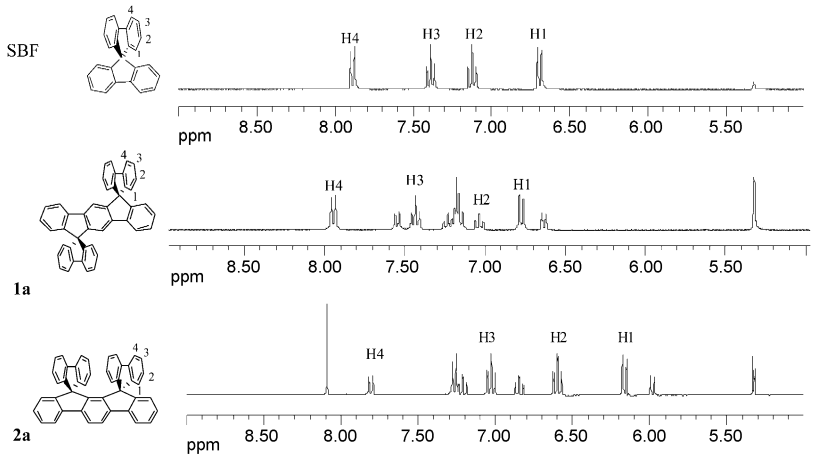

Figure 2. Low field portion of the ^{1}H NMR spectra (CD_2Cl_2) of **SBF**, **1a** and **2a**.

effect may be assigned to the increased overlap of the aromatic rings of the two face-to-face fluorene units, found in **2a**. Indeed, despite the structural differences between the two central cores, that is, (1,2-*b*)-IF and (2,1-*a*)-IF, we have shown that all the hydrogen atoms of the cores show almost identical ^{1}H NMR chemical shifts (see above, Table S1). It is hence reasonable to assume that the shielding of the hydrogen atoms borne by the fluorene units, in **2a**, results from their face-to-face geometry and not from their different indenofluorenyl central core. Indeed, transannular π–π interactions are usually accompanied by high field shifts in ^{1}H NMR spectra[9,32–35] and have been observed in different systems such as for example acridylnaphthalene,[32] paracyclophane,[35] polyfluorene,[9,34] thiophene derivatives[15] and tetrapyrenyl compounds.[36] The *t*Bu-substituted derivatives **1b** and **2b** rigorously present the same behavior as that reported above for **1a** and **2a** (Table S2). The highest chemical shift differences, $\delta_{1a}-\delta_{2a}$ and $\delta_{1b}-\delta_{2b}$, are always found for the hydrogen atom H4, about 0.65/0.68 ppm, which is therefore the hydrogen atom the most influenced by the π–π interactions.

In order to confirm the preliminary results obtained with non-aryl-substituted **1a/2a** and **1b/2b**, a similar ^{1}H NMR study was then performed on the aryl-substituted DSF-IFs series. In this context, the spirobifluorene derivative **m1**, has been prepared as a relevant model compound of **1f/2f** (Scheme 2). Indeed, the model compound **m1** can be considered as a "half molecule" of both isomers **1f/2f** and should provide relevant information about the influence of the two face-to-face fluorene units in the DSF-IFs **2**. In the ^{1}H NMR spectrum of **m1**, the chemical shifts of the hydrogen atoms of the fluorene unit, that is, H1, H3, H4 and those of the (4-nonylphenyl) units, that is, H10 and H11, were almost identical to those of their homologues in **1f** (Table S3). This feature clearly evidences that, "aryl-fluorene-aryl" moieties in **1f** and in **m1** are in a very similar chemical environment.

A significantly different behavior is observed for the isomer **2f** since all the signals of the hydrogen atoms of its "aryl-fluorene-aryl" moieties are strongly deshielded compared with those in **1f** (Table S3). This shielding effect observed in **2f** is assigned to intramolecular π–π interactions between face-to-face "aryl-fluorene-aryl" units. The same trend is observed for all the other couples of isomers, that is, **1c–g/2c–g** (exemplified in Figure 3 with **1d/2d**). Indeed, the hydrogen atoms signals of the "aryl-fluorene-aryl" moieties are always shielded for each isomer **2** compared to its congener **1**. For the fluorene units, the maximum chemical shift difference between two isomers is always found for H4 (ca. 0.5 ppm) and for the aryl rings, the maximum chemical-shift difference is always found for H10 (around 0.4 ppm, Table S3 in the Supporting Information). H10 and H4 are hence the hydrogen atoms which are the most influenced by the π–π interactions of "aryl-fluorene-aryl" moieties.

To conclude, an upfield shift for the "aryl-fluorene-aryl" hydrogen atoms signals of all DSF-IFs **2** is observed compared to those of DSF-IFs **1**. In the light of this detailed and comparative ^{1}H NMR study, we can unambiguously conclude that, in **2c–g**, π–π interactions occur between the two cofacial "aryl-fluorene-aryl" moieties. Furthermore, this study gives important structural information as it highlights

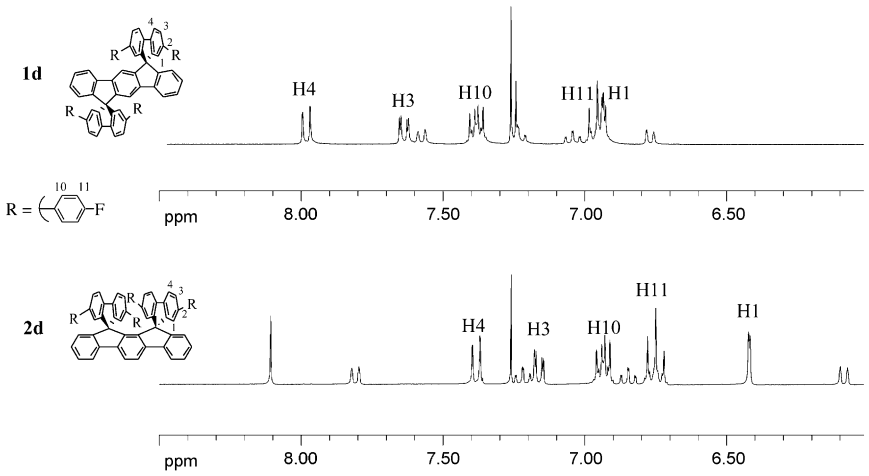

Figure 3. Low field portion of the ^{1}H NMR spectra ($CDCl_3$) of **1d** and **2d**.

that H10 and H4 are the hydrogen atoms which are the most influenced by this effect. Such π–π interactions between the "aryl-fluorene-aryl" moieties in **2c**–**g** should lead to significantly different electrochemical and optical properties compared to their isomers **1c**–**g** as discussed next.

Electrochemical properties

The redox properties of all compounds were investigated by cyclic voltammetry (CV), differential pulse voltammetry (DPV) and selected data are summarized in Table 1 (**1c**–**f**/**2c**–**g** CVs and DPVs are provided in the Supporting Information, Figures S5–S13).

Compounds **1a** and **2a**,[2] constituting building blocks of aryl-substituted DSF-IFs **1c**–**g** and **2c**–**g**, present HOMO levels at about −5.76 and −5.64 eV and LUMO levels at about −2.17 and −2.03 eV, respectively. These HOMO/LUMO levels are mainly controlled by the indenofluorenyl core and also slightly affected by the arrangement of the fluorene units (face-to-face in **2a** or not face-to-face in **1a**).[31] Indeed, (1,2-*b*)-IF and (2,1-*a*)-IF present identical HOMO level values lying at about −5.6 eV. For **1a**, the HOMO level is lowered by 0.15 eV compared to (1,2-*b*)-IF, whereas for **2a**, the HOMO level is almost identical to that of (2,1-*a*)-IF. This difference may be due to a less effective withdrawing effect of the two face-to-face fluorene units in **2a** when compared to the withdrawing effect of the two independent fluorenes in **1a**.[31]

Surprisingly, the HOMO levels of **1c**–**f** (-5.59 ± 0.17 eV) are always found at lower energy than the HOMO levels of their isomers **2c**–**f** (-5.41 ± 0.08 eV). The HOMO energy levels of **1c**–**f** span a very small range (−5.49 eV for **1c** to −5.73 eV for **1d**) and are all slightly higher than the HOMO level of **1a** (−5.76 eV).[31] Similarly, the HOMO energy levels of **2c**–**g**, also span a small range (−5.33 eV for **2c** to −5.50 eV for **2d**) and are all higher than the HOMO level of **2a** (−5.64 eV). Compared to **1a**, HOMO levels of

[2] Electrochemical properties of **1a** and **2a** have been previously reported.[26,31]

Table 1. Selected electrochemical and optical data of DSF-IFs **1** and **2**.

	E_{ox} [V]	E^{ox}_{onset} [V]	E^{red}_{onset} [V]	HOMO [eV][a]	LUMO [eV][b]	LUMO [eV][c]	ΔE^{El} [eV][d]	ΔE^{opt} [eV][e]
(1,2-*b*)-IF[31]	1.31 ($1e^-$), 2.01 ($>1e^-$)	1.21	−2.41	−5.61	−1.99	−2.00	3.62	3.61
(2,1-*a*)-IF[31]	1.31 ($1e^-$), 1.98 ($>1e^-$)	1.22	−2.46	−5.62	−1.94	−1.86	3.68	3.76
1a	1.47 ($1e^-$), 1.95[f] ($>1e^-$)	1.36	−2.23	−5.76	−2.17	−2.25	3.59	3.51
2a	1.36 ($1e^-$), 1.69 ($1e^-$), 1.99 ($>1e^-$)	1.24	−2.37	−5.64	−2.03	−2.07	3.61	3.57
1c	1.28 ($3e^-$), 1.53[f] ($2e^-$), 1.75 ($1e^-$), 1.96 ($2e^-$)	1.09	−2.40	−5.49	−2.00	−2.04	3.49	3.45
2c	1.07 ($2e^-$), 1.31($1e^-$), 1.51 ($2e^-$), 1.63 ($2e^-$), 1.93 ($1e^-$)	0.93	−2.42	−5.33	−1.98	−1.94	3.34	3.39
1d	1.45 ($1e^-$), 1.55 ($1e^-$), 1.66 ($1e^-$), 1.87[f] ($>1e^-$), 1.96 ($>1e^-$)	1.33	−2.24	−5.73	−2.16	−2.24	3.57	3.49
2d	1.20 ($1e^-$), 1.36 ($1e^-$), 1.58 ($1e^-$), 2.06[f] ($>1e^-$)	1.10	−2.39	−5.50	−2.01	−2.06	3.49	3.44
1e	1.42 ($1e^-$, shoulder), 1.70 ($>1e^-$)	1.17	−2.4	−5.57	−2.00	−2.08	3.57	3.49
2e	1.13 ($1e^-$), 1.31 ($1e^-$), 1.57 ($1e^-$), 1.97 ($2e^-$)	1.02	−2.4	−5.42	−2.00	−2.02	3.42	3.40
1f	1.30 ($1e^-$), 1.38 ($1e^-$), 1.68 ($2e^-$), 2.13[f] ($>1e^-$)	1.19	−2.33	−5.59	−2.07	−2.11	3.52	3.48
2f	1.11 ($1e^-$), 1.25 ($1e^-$), 1.60 ($1e^-$), 1.87 ($>1e^-$), 2.02[f] ($>1e^-$)	1.01	−2.38	−5.41	−2.02	−2.01	3.39	3.40
1g								3.50
2g	1.10 ($1e^-$), 1.32 ($1e^-$), 1.73 ($1e^-$), 1.96 ($>2e^-$)	0.99	−2.44	−5.39	−1.96	−1.92	3.43	3.47

[a] Calculated from the onset oxidation potential E^{ox}_{onset}.[37] [b] Calculated from the onset reduction potential E^{red}_{onset}.[37] [c] Calculated from the HOMO energy level and the edge of optical band gap. [d] Calculated as $\Delta E^{El} = |\text{HOMO–LUMO}|$ from redox data. [e] Optical band gap $\Delta E^{opt} = hc/\lambda$ (ΔE^{opt} [eV] = 1237.5/λ) has been estimated from the liquid UV/Vis spectra in THF. [f] Beginning of the electropolymerization process observed along recurrent sweeps.

1c–f (except **1d**) are shifted by at least 0.17 eV. Similarly, compared to **2a**, the HOMO levels of **2c–g** (except **2d**) are shifted by at least 0.22 eV. These observations led us to conclude that the HOMO levels of aryl substituted **1c–f** and **2c–g** are not only governed by the electronic properties of the central indenofluorenyl core but also i) by the presence of the "aryl-fluorene-aryl" units and ii) by the geometry of the indenofluorenyl core which leads to "aryl-fluorene-aryl" units in different structural environment (face-to-face in DSF-IFs **2** or not face-to-face in DSF-IFs **1**). In addition, it is important to stress that the HOMO energy levels of **1c–f** and **2c–g** can be finely tuned depending on the substituents borne by the aryl rings. Indeed, **1d**/**2d** for example, present low-lying HOMO levels (**1d**: −5.73 eV and **2d**: −5.50 eV), significantly different from those of their congeners and assigned to the electron-withdrawing effect of the fluorine atoms borne by the aryl rings.

In the cathodic range (see Figures S5–S13 in the Supporting Information), all aryl-substituted **1c–f** and **2c–g** exhibit an irreversible reduction wave, which maximum is not observed before the reduction of the electrolytic medium (CH_2Cl_2; 0.2 M $[NBu_4][PF_6]$). However, the CVs allowed the determination of the reduction onset potential (E^{red}_{onset}) and hence to the LUMO energy levels. Thus, all compounds present LUMO levels, close to −2.0 eV (−2.08 ± 0.08 eV for **1c–f** and −2.00 ± 0.04 eV for **2c–g**). The LUMO energy levels of **1c–f** and **2c–g** are almost identical to those of their corresponding parent indenofluorenes (−1.99 eV for (1,2-*b*)-IF and −1.94 eV for (2,1-*a*)-IF, Table 1). The very low LUMO energy levels of **1c–f** and **2c–g** highlight their poor electron-affinities.

The electrochemical band gaps ΔE^{El} (consistent with the measured optical band gaps ΔE^{opt}, Table 1) of both **1c–f** and **2c–g** are wide (ca. 3.3/3.6 eV) and dependent of the substituents borne by the aryl groups. The band gaps of **1c–f** (around 3.5/3.6 eV) are always larger compared to those of their corresponding isomers **2c–g** (3.3/3.5 eV) due to the higher HOMO levels of **2c–g**. Compared to its constituting building block **1a** ($\Delta E^{El} = 3.59$ eV), **1c–f** present a similar band gap, around 3.5/3.6 eV. A drastically different behavior is observed with **2c–g**, which present a smaller band gap (3.3/3.5 eV) compared to its building block **2a** ($\Delta E^{El} = 3.61$ eV). Careful investigations of these intriguing different electrochemical behaviors between **1c–f** and **2c–g** are disclosed below.

Aryl-substituted **1c–f**, present a first oxidation potential E^1_{ox} ranging from 1.28 V for **1c** to 1.45 V for **1d**. This might be easily rationalized by the electron-donating/electron-withdrawing effects of the different substituents borne by the phenyl rings. Thus, **1c** with three electron-donating methoxy groups on the phenyl rings present the lowest E^1_{ox} (1.28 V, Table 1) of the series. On the contrary **1d**, with an electron-withdrawing fluorine atom on the phenyl rings, presents the highest E^1_{ox} (1.45 V, Table 1) of the series. Thus, E^1_{ox} can be easily tuned by the nature and the position of the different substituents borne by the phenyl rings.

An important feature in **1c–f** is to assign the different electron transfers. The assignment of the first electron transfer, indenofluorenyl versus "aryl-fluorene-aryl" cores oxidation, appears however difficult to perform. Indeed, **1a** the constituting building block of **1c–g** presents a first oxidation wave E^1_{ox} at 1.47 V that is assigned to an indenofluorenyl electron transfer.[26] On the other hand, literature reports for several molecules bearing the "aryl-fluorene-aryl" moieties such as 2,7-bis-(4-*tert*-butylphenyl)-9,9′-spirobifluorene[38] and 2,2′,7,7′-tetraphenyl-9,9′-spirobifluorene,[39] a first oxidation potential E^1_{ox} around 1.39 V vs SCE. It is hence difficult to assign the first electron transfer of **1c–f** since i) the indenofluorenyl core and the "aryl-fluorene-aryl" core are oxidized at similar potentials (1.47 vs 1.39 V, respectively) and ii) **1c–f** present a first oxidation potential E^1_{ox} ranging from 1.28 to 1.45 V, depending on the substituents borne by the phenyl rings. We thus focus on a single illustrative example with identical phenyl rings substitution, namely **1f** and its model compound **m1**, both bearing a nonyl chain in *para*-position of the phenyl rings (Figure S11 and S14 in the Supporting Information). This example has been chosen since the nonyl chains i) allow a very good solubility of both **1f** and **2f** and ii) do not add any strong electronic effect. Thus, **m1** possesses a first multielectronic oxidation wave at about 1.45 V corresponding to the oxidation of the "aryl-fluorene-aryl" moieties, consistent with the calculated nature of its HOMO (Figure S29 in the Supporting Information). In addition, **1f** presents a first oxidation E^1_{ox} at 1.30 V (vs. 1.45 V for **m1**). On the basis of the oxidation potentials of **1f** and **m1**, it is then reasonable to contend that the first oxidation process in **1f** leans more towards the (1,2-*b*)-indenofluorenyl core than to the "aryl-fluorene-aryl" moieties. Theoretical calculations on **1d–g** models lend support to this assignment with the following nuances: the calculated nature of their HOMOs shows that they are spread out between both types of electrophores with a strong contribution of the indenofluorenyl moiety (see Figures S24–S28). It should be noted that **1c**, bearing three methoxy groups per phenyl unit appears in the series as an exception. Indeed, **1c** has a HOMO level fully centered on the "aryl-fluorene-aryl" units due to the strong electron-donating effect of its methoxy groups.

Compounds **1c–f** present a second oxidation potential E^2_{ox} ranging from 1.28 V for **1c**[3] to 1.70 V for **1e**. Notably, **1f** presents a second oxidation potential E^2_{ox} recorded at 1.38 V. This potential is close to that of the first of the model compound **m1** (1.45 V, see above). As the first oxidation process in **1f** has been assigned to an orbital with a strong indenofluorenyl character (see above), it is hence rational to assign the second oxidation process of **1f** to the oxidation of an "aryl-fluorene-aryl" moiety. We contend that aryl-substituted **1c–g** possess the same behavior. Accordingly, theoretical calculations on **1c–f** models indicate that their SOMOs are all strongly centered on the "aryl-fluorene-aryl" moieties (see Supporting Information). In the light of these two ob-

[3] Oppositely to **1d–f**, we note that the first wave of **1c** (1.28 V) is multielectronic and hence the oxidation of both the indenofluorenyl core and the "aryl-fluorene-aryl" moieties occurs at very close potentials.

servations, one can then conclude that **1d–f** are sequentially oxidized with a first oxidation process centered on a site with a strong (1,2-*b*)-indenofluorenyl character and a second oxidation centered on the "aryl-fluorene-aryl" moieties. As exposed above, **1c** appears as an exception with both HOMO and SOMO fully located on the "aryl-fluorene-aryl" moieties.

Aryl-substituted **2c–g** present a first reversible oxidation wave E^1_{ox} around 1.1 V (from 1.07 V for **2c** to 1.20 V for **2d**). As exposed above with **1c–g**, the first oxidation potential of **2c–g** is slightly shifted depending of electron-donating/electron-withdrawing effects of the different substituents borne by the phenyl rings. However, the key feature is related to the marked difference observed between the first oxidation potentials of **2c–g** and those of **1c–g**. Indeed, all aryl-substituted **2c–g** are oxidized at a significantly lower potential than their corresponding isomers **1**. As the first oxidation of **2a**, constituting building block of **2c–g**, is observed at 1.36 V and centered on the (2,1-*a*)-indenofluorenyl core,[31] the first oxidation of **2c–g** (around 1.1 V) is probably not centered on the (2,1-*a*)-indenofluorenyl core. However, this first and reversible oxidation wave of **2c–g** is not centered either on the "aryl-fluorene-aryl" moieties, which are found at higher potentials values (vide supra). The "aryl-fluorene-aryl" cofacial arrangement in **2c–g** is hence at the origin of their remarkably low first oxidation potential, as it is known that the oxidation of π-stacked systems is more facile than their non-stacked analogues.[34,40] It is hence rational to assign the first oxidation process of **2c–g** to an oxidation centered on an "aryl-fluorene-aryl" cofacial dimer. This is confirmed by theoretical calculations, which show that the HOMO of **2c–g** has a mixed character with nevertheless major coefficients found on the "aryl-fluorene-aryl" moieties (see Supporting Information, Figures S24–S28).

The second oxidation process of **2c–g** is recorded at about 1.3 V, very similar to the first electron transfer of **2a** centered on the (2,1-*a*)-indenofluorenyl core and recorded at E^1_{ox} = 1.36 V, Table 1.[26] The second oxidation process of **2c–g** appears however to be highly dependent of the substituents borne by the phenyl rings. Indeed, theoretical calculations show that the SOMO of $\mathbf{2d}^{\bullet+}$, involved in the second monoelectronic oxidation, is almost exclusively centered on the (2,1-*a*)-indenofluorenyl core.[24] On the contrary, the calculated SOMO of $\mathbf{2f}^{+}$ is found to be spread out over the two types of electrophores with nevertheless a strong indenofluorenyl character, while in $\mathbf{2c}^{\bullet+}$, $\mathbf{2e}^{\bullet+}$ and $\mathbf{2g}^{\bullet+}$ the SOMOs are found to be mainly centered on the "aryl-fluorene-aryl" moieties (see Supporting Information). This is tentatively attributed to the effect of the strongly electron-donating phenyl substituents in **2c**, **2e** and **2g**.

Interestingly, with the exception of **1e**/**2e**, the shift between the two first oxidation waves ($E^2_{ox}-E^1_{ox}$) is always larger in **2c–f** compared to **1c–f**. This potential difference shows that the radical cations of **2c–f** is significantly more stabilized thermodynamically compared to those of **1c–f**. This difference between the two series might be ascribed to the different character of their HOMO levels induced by their different geometry profiles. Indeed and as exposed above, theoretical calculations show for **1c–f** a HOMO almost exclusively centered on the indenofluorenyl core, as opposed to the "aryl-fluorene-aryl" moieties character observed for the HOMO level of **2c–f** (see Supporting Information). Thus, the oxidation of **1c–f** leads to a radical cation where the cationic charge is delocalized on the (1,2-*b*)-indenofluorenyl core whereas the oxidation of **2c–f** results in a radical cation where the cationic charge is delocalized over both "aryl-fluorene-aryl" moieties. Therefore, the radical cations of **2c–f** appear to be much more stabilized compared to those of **1c–f**.

To conclude, the electrochemical investigations of aryl-substituted DSF-IFs **1c–g** and **2c–g** have highlighted the marked differences between these two families of molecules. Notably, in **2c–f**, the first oxidation process is always found at a lower potential compared to their congeners **1c–f** clearly signing the intramolecular π–π interactions of "aryl-fluorene-aryl" moieties in **2c–f**.

Optical properties in solution

Absorption spectroscopy: UV/Vis absorption spectrum of **1a** (THF) presents a fine vibronic structure with λ_{max} = 345 nm (Figure 4, top). Our previous works demonstrated that this band corresponds to the absorption of the (1,2-*b*)-indenofluorenyl chromophore.[26,41]

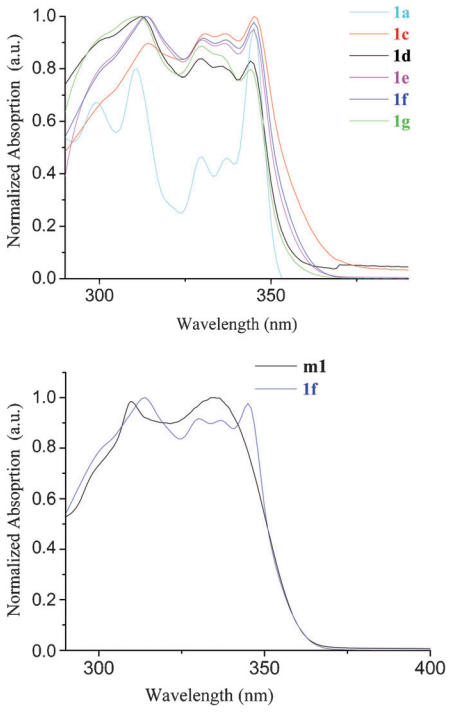

Figure 4. Absorption spectra (THF, $c = 10^{-6}$ M) of top: **1a** and **1c–g**; bottom: **1f** and the model compound **m1**.

Aryl-substituted **1c–g**, in solution in THF (Figure 4, top), present an absorption band in which, one can distinguish five maxima at about λ_{max} = 301 (shoulder), 314, 327, 336, and 345 nm. Despite the general broadness of these spectra, the five absorption bands fit well with those of **1a**, constituting building block of **1c–g**. The broadness of the **1c–g** spectra is due to a rotational freedom of the aryl rings around the C–C bonds joining the fluorene and the aryl units. The model compound **m1** gave us important insights on the assignments of the different electronic transitions. Thus, the UV/Vis spectrum of **m1** has two maxima at about λ_{max} = 310 and 335 nm, fitting well with its DSF-IF analogue **1f** (Figure 4, bottom). However, **m1** does not show any band at 345 nm, which was observed in the UV/Vis spectrum of **1f** and assigned to the (1,2-*b*)-indenofluorenyl core.[26,42] In addition, the band at about 314 nm and the split band at about 330–336 nm found in all aryl-substituted DSF-IFs **1c–g**, have been ascribed to the "aryl-fluorene-aryl" moieties. Indeed, these bands are also found in other oligoaryl derivatives linked by a central spirobifluorene unit as previously reported in the literature.[4,43,44]

The UV/Vis absorption spectra of DSF-IFs **2** were also studied in solution (Figure 5) and compared to those of DSF-IFs **1**. With respect to **1a**, the UV/Vis spectrum of **2a** exhibits a main absorption band slightly hypsochromically shifted by 4 nm (λ_{max} = 339 nm), in accordance with previous observations on the (1,2-*b*)-IF and (2,1-*a*)-IF core.[25,45] This hypsochromic shift, has been assigned to a better delocalization of π-electrons in **1a** compared to **2a**. The UV/Vis absorption spectra of aryl-substituted **2c–g** present broad bands, with two maxima at about 323 and 340 nm. It should be stressed that **2c** possess a broader spectrum compared to **2d–g**. The lowest energy transition at 340 nm is found for all aryl-substituted **2c–g** and fits well with that of **2a**. This transition has been hence ascribed to the (2,1-*a*)-indenofluorenyl core, similarly to the above discussion on the DSF-IF **1** molecules.

In addition, a salient feature is the absorption onset of **2c–g**, which is always found at higher intensity and wavelength than those of **1c–g**, respectively (Figure 5, bottom).[24] Similar features in the absorption spectra of other molecular systems containing two chromophores in a face-to-face arrangement, have been previously reported in the literature, and assigned to intramolecular interactions in the ground state.[10,13,46,47] These π–π interactions, in the ground state, between the two face-to-face "aryl-fluorene-aryl" units are in complete accordance with the results obtained in the ^{1}H NMR and electrochemical studies (see above). Moreover, the spectral features (red-shift, weak oscillator strength) of the onset observed in the absorption band of **2c–g** is consistent with the presence of H-aggregates, as depicted by Kasha for "side-by-side" interaction[48] of the two "aryl-fluorene-aryl" transition dipole moments for S_0–S_1 excitation. It can be stressed that in compound **2a**, this interaction seems to be negligible, certainly due to the much smaller transition dipole moments of the unsubstituted fluorenes.

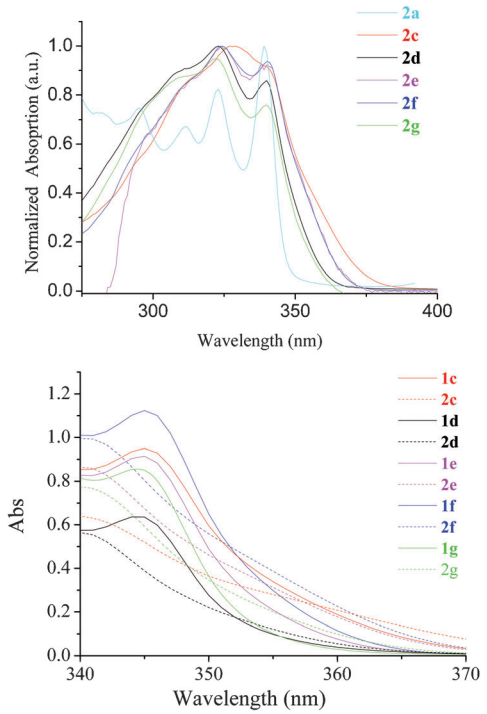

Figure 5. Top: Absorption spectra of **2a** and **2c–g** in solution in THF ($c = 10^{-6}$ M). Bottom: focus on the 340/370 nm portion of the absorption spectra of **1c–g** and **2c–g** (10^{-5} M in THF).

Fluorescence spectroscopy: The fluorescence spectrum (THF) of **1a** presents a fine vibronic structure with λ_{max} = 348 nm (Figure 6, top).[26] The fluorescence spectra of aryl-substituted **1d–g** (Figure 6, top, Table 2) display two well-defined bands in the near UV domain, that is, at 360/368 and 377/385 nm. Thus, the first emission peak of **1d–g** (360/368 nm) is red-shifted with respect to **1a** (348 nm) due to the important contributions of the aryl rings leading to a more conjugated excited state. This effect has been previously highlighted with indenofluorene derivatives.[42] This feature is also confirmed by the fluorescence spectra of **1d–g**, which are better resolved than their absorption spectra. Such differences between absorption and emission bandshapes could be related to the flexible character of the molecules, as already studied for *p*-terphenyl and indenofluorene compounds by ab initio quantum chemical methods.[49] This suggests that, in the excited state, the bonds joining the fluorene and the aryl rings acquire some double bond character, hence a more rigid/planar structure.[50] It should be noted that **1c** presents a different behavior with a less well-defined and red-shifted fluorescence spectrum compared to its analogues **1d–g**. This has been ascribed to the electron-donating effect of the methoxy groups borne by the pendant phenyl rings.[4,23,51] A fine tuning of the emission color in **1c–g** can be hence easily achieved using electron-donating or electron-withdrawing substituents.

The fluorescence spectrum of the model compound **m1**, is identical in shape to that of its homologue **1f** (Figure 6

Table 2. Optical properties of DSF-IFs **1** and **2**.

	λ_{abs}[a] liq [nm]	λ_{abs}[b,g] film [nm]	$\lambda_{em\ liq}$[c] [nm]	λ_{em}[d,g] film [nm]	$\lambda_{em}-\lambda_{abs}$ liq [nm]	ϕ_{sol}[e] (%)
(1,2-*b*)-IF[31]	289, 302, 319, 328, 334	f	339, 347, 356	f	5	61
(2,1-*a*)-IF[31]	307, 315, 322	f	326, 343, 360	f	4	60
1a[31]	299, 310, 328, 336, 345	301, 313, 332, 340, 349	348, 355, 366, 388 (sh) , 405 (sh)	355, 374, 386	3	62
2a[31]	295, 311, 323, 339	300, 314, 323, 339	345, 363, 380 (sh) , 400 (sh)	–	6	60
1b	294, 302, 314, 330, 338, 346	305 (sh), 316, 333, 340, 350	350, 368, 390 (sh), 410 (sh)	374, 394, 415 (sh)	4	70
2b	295, 307, 323, 340	285, 298 (sh), 308, 320, 326, 344	346, 365, 382 (sh) , 404 (sh)	350, 369, 388, 408 (sh)	6	68
1c	301 (sh), 314, 331, 337, 345	303 (sh), 317, 332, 341, 351	381 (sh), 393	416	36	75
2c	314 (sh), 328, 340	314 (sh), 332, 345	457	466	116	35
1d	301 (sh), 313, 330, 336, 345	301 (sh), 316, 333, 341, 349	360, 377, 397 (sh), 417 (sh)	387, 401, 423, 448 (sh)	15	77
2d	311 (sh), 323, 340	312 (sh), 329, 345	450	451	110	30
1e	301 (sh), 314, 330, 336, 345	f	365, 384, 403 (sh), 426 (sh)	f	20	77
2e	311 (sh), 324, 340	312 (sh), 326, 343	413	432	73	48
1f	301 (sh), 314, 330, 337, 345	303 (sh), 317, 332, 340, 349	368, 385, 406 (sh), 432 (sh)	377, 392, 411, 441 (sh)	23	77
2f	312 (sh), 324, 340	315 (sh), 327, 345	454	453	114	30
1g	303 (sh), 312, 329, 334, 344	f	363, 380, 399(sh), 423 (sh)	f	19	74
2g	310 (sh), 322, 340	310, 324, 342	404 (sh), 431	434	64	38
m1	310, 335	–	366, 384	–	31	75

[a] Absorption spectra in solution in THF ($c=10^{-6}$ M). [b] Absorption spectra in thin-solid films (depositing solvent: toluene: **1a**; 1,2-dichlorobenzene (1,2-DCB): **2a**, **1c**/**2c**; THF: **1d**, **1f**, **1b**/**2b**, **2d**–**g**. $c=15\ mg\,mL^{-1}$ or $10\ mg\,mL^{-1}$). [c] Emission spectra in solution in THF ($c=10^{-6}$ M) with $\lambda_{exc}=345$ nm for DSF-IFs **1** and $\lambda_{exc}=340$ nm for DSF-IFs **2**. [d] Emission spectra in thin-solid films (depositing solvents: toluene: **1a**; 1,2-DCB: **1c**/**2c** THF: **1d**, **1f**, **1b**/**2b**, **2d**–**g**. [e] The relative quantum yield was measured with reference to quinine sulfate in 1 N H_2SO_4 ($\phi=0.546$). [f] Not recorded due to very poor solubility. [g] Spectra provided in the Supporting Information.

inset, top). Since the quantum yields (Table 2) and molar absorption coefficients (see Table S4 in the Supporting Information) of **1f** and **m1** are almost identical, it is reasonable to conclude that the main fluorescent emitter in **1f** is the "aryl-fluorene-aryl" moieties. The emission maxima of **1d**–**g** are also in perfect accordance with those previously reported in the literature for fluorophores containing "aryl-fluorene-aryl" units.[21,38,43,44] Similarly, the fluorescence of **1c**–**g** appears hence to be mainly due to the emission of the "aryl-fluorene-aryl" fluorophores. This is also confirmed by the considerable difference observed between non aryl derivatives **1a**–**b** and aryl derivatives **1c**–**g**, in terms of molar absorption coefficients (see Supporting Information) and quantum yields (see Table 2).

The Stokes shifts[4] for **1c**–**g** are rather small and consistent with a rather rigid molecular structure (Table 2). However, these Stokes shifts are larger than those observed for the non-aryl **1a** and **1b** (3/4 nm). This difference in term of Stokes shift between non-aryl **1a**–**b** and aryl-substituted **1c**–**g** has been ascribed to i) the rotational freedom induced by the introduction of the aryl arms in **1c**–**g**, which leads to a loss of the rigidity and hence a larger Stokes shift and ii) the different fluorescent emitters that is, the indenofluorenyl core in the case of non-aryl **1a**–**b** and the "aryl-fluorene-aryl" moieties in the case of aryl-substituted **1c**–**g**.

The fluorescence spectra of DSF-IFs **2** were also studied in solution in THF (Figure 6, bottom, Table 2). **2a** presents two well-resolved emission bands at 345 and 363 nm assigned to the emission of the (2,1-*a*)-indenofluorenyl core.[31] Interestingly, the emission spectra of **2c**–**g** are significantly different than that of **2a** and than those of their corresponding isomers **1c**–**g** (Figure 6, top). Indeed, **2c**–**g** present a structureless and red-shifted band (with respect to **1c**–**g** and **2a**) with maxima recorded at 457 nm (**2c**), 450 nm (**2d**), 413 nm (**2e**), 454 nm (**2f**) and 404/431 nm (**2g**) (Figure 6, bottom). In addition and opposite to **1c**–**g**, the Stokes shifts of **2c**–**g** become very large (Table 2) highlighting the remarkable effect of the cofacial fluorenes arrangement found in **2c**–**g**. It is hence reasonable to contend that the fluorescence features of **2c**–**g** arise from intramolecular excimers, due to the interactions between "aryl-fluorene-aryl" moieties in the excited state. Several groups have also reported similar behavior in fluorescence spectroscopy, for example with oligophenyl based cruciforms,[7] ethynyltriphenylene derivatives,[8] dibenzofulvene polymers with fluorene side chains,[9] carbazolophanes,[10] and various pyrene derivatives.[6,12–14] It is hence clear that π–π interactions exist in **2c**–**g** not only in the ground state but are also strongly en-

[4] Defined in this work as $\lambda_{em}-\lambda_{abs}$ in nm.

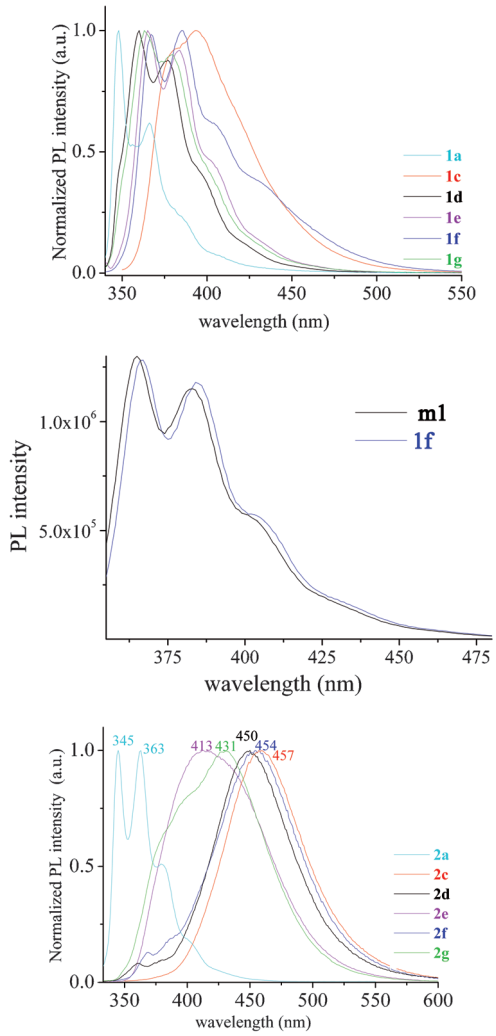

Figure 6. Top: Emission spectra ($\lambda_{exc}=345$ nm; $C=10^{-6}$ M in THF) of: **1a** and **1c–g**; middle: Emission spectra **1f** and **m1**. Bot1,tom: Emission spectra of **2a** and **2c–g** in THF ($\lambda_{exc}=340$ nm).

hanced in the excited state. These interactions in **2c–g** lead to drastically different emission colors compared to their positional isomers **1c–g**.

There are additional evidences for the assignment of the emission band of **2c–g** to the excimer formation upon intramolecular interactions of the "aryl-fluorene-aryl" fluorophores and not upon intermolecular interactions: i) the fluorescence spectra of **2c–g** are independent of the concentration (see Figure S15 for **2c** and S16 for **2e**) and ii) the fluorescence spectra of **2c–g** in solution are almost identical to those in solid state (see Figure S23). Such a behavior clearly signs that the fluorescence in **2c–g** arises from intramolecular excimer and not from intermolecular excimers.[52] A similar behavior has been recently highlighted by Meinardi and co-workers with oligothiophene derivatives.[18] It is also important to mention that the fluorescence of **2c–g** is independent of the excitation wavelength.

In terms of quantum yield (determined by standard method with quinine sulfate in H_2SO_4, see Supporting Information), aryl-substituted **1c–g** possess higher quantum yields (ca. 75%) than that observed for **1a** (ca. 62%)[26] due to the different emitters involved: the indenofluorenyl core in the case of non-aryl **1a** and the "aryl-fluorene-aryl" moieties in the case of aryl-substituted **1c–g**.

Whereas the quantum yield of **2a** is relatively high (ca. 60%),[31] we note an important decrease of the quantum yields in the case of aryl-substituted **2c–g** (30/48%) compared to **1c–g**. Therefore, the introduction of the aryl arms in **2c–g** has a remarkable effect not only on the emission color (Figure 6, bottom) but also on the quantum yields, which is consistent with the presence of H-type interaction of the two "aryl-fluorene-aryl" in addition to the intramolecular excimers in the case of **2c–g**.[7,11,53,54]

Finally, in **2c–g**, the emission color can be also easily tuned by the careful choice of the steric bulk of the substituent borne by the aryl rings. Indeed, **2c**, **2d** and **2f** present very similar, i) emission bands with maxima around 450 nm, ii) quantum yields, around 30%, iii) Stokes shifts, around 110 nm (Table 2). However, **2e** and **2g**, present drastically different behaviors as they possess i) the smallest Stokes shift that is, 73 nm (**2e**) and 64 nm (**2g**), ii) the highest quantum yield that is, 48% (**2e**) and 38% (**2g**) and iii) the shortest emission wavelengths that is, 413 nm (**2e**) and 431 nm (**2g**) in the series. The fluorescence spectra of **2e** and **2g** are hence significantly different compared to those of **2c**, **2d** and **2f**. This has been ascribed to a larger steric hindrance between the aryl rings induced by the bulkiness of the *tert*-butyl substituents borne by **2e** and **2g**. This steric hindrance in **2e** and **2g** leads to weaker π–π interactions between the "aryl-fluorene-aryl" moieties and hence compared to **2c**, **2d** and **2f**, to a shift of the emission band to shorter wavelength and to a higher quantum yield. This has been supported by theoretical modeling (see below). The bulkiness of the substituents borne by the aryl rings play hence a crucial role in the tuning of the emission color of aryl-substituted **2c–g**.[55] Such remarkable tuning of the emission band by steric hindrance appears to be a simple and efficient way to tune the emission colors of aryl-substituted DSF-IFs **2** fluorophores.

Fluorescence decays: In order to go deeper in the photophysical properties, the fluorescence decays of **1a–g** and **2a–g** were investigated in THF by the time-correlated single photon counting technique, with a common excitation wavelength at 330 nm (third harmonics of a fs-pulsed Ti/Sa laser). For each molecule, several decay curve acquisitions were performed at multiple emission wavelengths, in order to probe the properties in the blue edge, red edge, and in the middle region of the emission spectrum. The full sets of wavelength-dependent decay curves relative to single compounds were successfully analyzed by means of a global fitting procedure involving a single exponential (**1a–g**, **2a–b**) or three exponentials (**2c–g**). In all cases, satisfactory fits were obtained (global $\chi_R^2 < 1.2$, see Table 3).

Table 3. Fitting parameters of fluorescence decays (τ_i, A_i), fluorescence quantum yields Φ_F, radiative and non-radiative rates (k_r, k_{nr}) of DSF-IFs **1** and **2**.

	λ_{em}[a] [nm]	τ_1 [ns]	τ_2 [ns]	τ_3 [ns]	A_1 (f_1[b])	A_2 (f_2[b])	A_3 (f_3[b])	χ^2_r[c]	Φ_F	k_r[g] ($\times10^8$ s^{-1})	k_{nr}[g] ($\times10^8$ s^{-1})
	350										
1a[d]	375	1.95	–	–	1.00	–	–	1.18	0.62	3.2	1.9
	400				(1.00)						
	350										
1b[d]	375	1.96	–	–	1.00	–	–	1.06	0.70	3.6	1.5
	400				(1.00)						
	375										
1c[d]	400	1.17	–	–	1.00	–	–	1.15	0.75	6.4	2.1
	425				(1.00)						
	450										
	350										
1d[d]	375	1.34	–	–	1.00	–	–	1.12	0.77	5.8	1.7
	400				(1.00)						
	375										
1e[d]	400	1.10	–	–	1.00	–	–	1.14	0.77	7.0	2.1
	425				(1.00)						
	375										
1f[d]	400	1.09	–	–	1.00	–	–	1.12	0.77	7.1	2.1
	425				(1.00)						
	350										
1g[d]	375	1.24	–	–	1.00	–	–	1.10	0.77	6.2	1.9
	400				(1.00)						
(1,2-*b*)-IF[e]	350	1.54	–	–	1.00	–	–	1.20	–	–	–
					(1.00)						
(2,1-*a*)-IF[e]	350	1.25	–	–	1.00	–	–	0.99	0.61	4.9	3.1
					(1.00)						
	350										
2a[d]	375	2.08	–	–	1.00	–	–	1.17	0.60	2.9	1.9
	400				(1.00)						
	350										
2b[d]	375	1.83	–	–	1.00	–	–	1.18	0.68	3.7	1.8
	400				(1.00)						
	375				0.15	0.11	0.74				
					(0.91)	(0.08)	(0.01)				
	425				0.25	0.12	0.63				
					(0.94)	(0.05)	(0.01)				
2c[f]	475	11.25	1.30	0.035	0.39	0.12	0.49	1.10	0.35	–	–
					(0.96)	(0.03)	(0.01)				
	525				0.53	0.10	0.37				
					(0.98)	(0.02)	(0.00)				
	350				0.07	0.10	0.83				
					(0.87)	(0.12)	(0.01)				
	400				0.17	0.11	0.72				
					(0.94)	(0.06)	(0.00)				
2d[f]	450	12.99	1.28	<0.030	0.33	0.11	0.56	1.03	0.30	–	–
					(0.97)	(0.03)	(0.00)				
	500				0.52	0.08	0.40				
					(0.98)	(0.02)	(0.00)				
	350				0.23	0.07	0.70				
					(0.93)	(0.05)	(0.02)				
	400				0.29	0.06	0.65				
					(0.95)	(0.03)	(0.02)				
2e[f]	450	7.56	1.19	0.074	0.36	0.06	0.58	1.03	0.48	–	–
					(0.96)	(0.03)	(0.01)				
	500				0.46	0.05	0.49				
					(0.97)	(0.02)	(0.01)				
	360				0.10	0.11	0.79				
					(0.87)	(0.09)	(0.04)				
	400				0.15	0.10	0.75				
					(0.92)	(0.06)	(0.02)				
2f[f]	450	11.16	1.04	0.070	0.25	0.09	0.66	1.09	0.30	–	–
					(0.95)	(0.03)	(0.02)				
	500				0.38	0.07	0.55				
					(0.97)	(0.02)	(0.01)				

Fluorescence decay curves of **1a–g** (Figure 7, top) were found to be monoexponential and insensitive to emission wavelength, with lifetimes measured at 1.95–1.96 ns for non aryl-substituted **1a–b** and comprised between 1.09 ns and 1.34 ns for aryl-substituted **1c–g**. The marked difference between the lifetimes of **1a–b** and those of **1c–g** (Figure 7, Table 3) clearly evidences that the emission arises from different molecular species: the indenofluorenyl core in the case of non aryl-substituted **1a–b**, and the "aryl-fluorene-aryl" moieties in the case of aryl-substituted **1c–g**. This general conclusion is fully compatible with the analysis of the related absorption and fluorescence spectra, as discussed above. Furthermore, this scheme is in perfect accordance with the lifetime of a pure spiro "aryl-fluorene-aryl" analogue reported by Salbeck and coworkers, which was found to be ~1.1 ns in dichloromethane[4] and with the lifetime of the core compound (1,2-*b*)-IF (1.54 ns, see Table 3).

For **1a–b**, the radiative (k_r) and non-radiative (k_{nr}) rate constants were calculated to be 3.2–3.6 $\times10^8$ s^{-1} and 1.5–1.9 $\times10^8$ s^{-1}, respectively. Interestingly, the **1c–g** derivatives show similar non-radiative rate constants ($k_{nr}=1.7$–2.1×10^8 s^{-1}), but k_r is more than doubled ($k_r=5.8$–7.1×10^8 s^{-1}). The higher quantum yields and shorter lifetimes of the "aryl-fluorene-aryl" derivatives **1c–g** are then mostly due to faster radiative deactivations compared to the indenofluorenyl species in the case of **1a–b**.

For **2a–b** compounds, the fluorescence decay curves were recorded and fitted satisfactorily with a single exponential (Figure 7, bottom, Figure 8, top, Table 3). The lifetimes were found to be in a very similar

Table 3. (Continued)

	λ_{em}[a] [nm]	τ_1 [ns]	τ_2 [ns]	τ_3 [ns]	A_1 (f_1[b])	A_2 (f_2[b])	A_3 (f_3[b])	χ^2_r[c]	Φ_F	k_r[g] ($\times10^8$ s^{-1})	k_{nr}[g] ($\times10^8$ s^{-1})
2g[f]	350	10.75	0.90	<0.030	0.05 (0.49)	0.58 (0.51)	0.37 (0.00)	1.04	0.38	–	–
	375				0.06 (0.55)	0.63 (0.45)	0.31 (0.00)				
	425				0.10 (0.66)	0.62 (0.34)	0.28 (0.00)				
	475				0.17 (0.76)	0.65 (0.24)	0.18 (0.00)				

[a] Selected emission wavelength by means of a monochromator with a 50 nm-bandwidth. [b] Intensity fractions were calculated by the following equation: $f_i = A_i\tau_i/\Sigma A_j\tau_j$ [c] Global χ^2_r, obtained for a global analysis of the full set of decay curves. [d] Excitation at 330 nm and fluorescence decay recorded on a 25 ns-time window (channel width = 6.1 ps, pulse fwhm = 47 ps). [e] Excitation at 310 nm and fluorescence decay recorded on a 25 ns-time window (channel width = 6.1 ps, pulse fwhm = 47 ps), including a long-pass filter to reduce the scattering signal. [f] Excitation at 330 nm and fluorescence decay recorded on two different time windows to reach a high degree of accuracy at both short and long time-ranges: 12.5 ns (channel width = 3.05 ps and pulse fwhm = 35 ps) and 100 ns (channel width = 24.4 ps, pulse fwhm = 102 ps). [g] Except for **2c–g**, k_r and k_{nr} were calculating assuming that: $\Phi_F = k_r/(k_r+k_{nr})$ and $1/\tau_1 = k_r + k_{nr}$.

range compared to **1a–b**: 2.08 ns (**2a**) and 1.83 ns (**2b**). The radiative and non-radiative rate constants are also very close to those determined for **1a–b** (see Table 3). Together with the short Stokes shift as already mentioned in a previous paragraph, this observation suggests that in the non-aryl DSF-IFs series (**1a–b** and **2a–b**), the emission predominantly arises from their central indenofluorenyl cores. The difference between **1a–b**/**2a–b** lifetimes and those of their corresponding core compounds (2,1-*a*)-IF (1.25 ns) and (1,2-*b*)-IF may originate from the electron-withdrawing effects of spirofluorene units.

The fluorescence decays of **2c–g** show a drastically different shape (Figure 7, bottom). Indeed, the decay curves are multiexponential and extend over 50 up to 100 ns (three decades). The analysis was performed with a sum of three exponentials. The first time-constant A_1 is very slow (7.5–13.0 ns), the second one A_2 is in

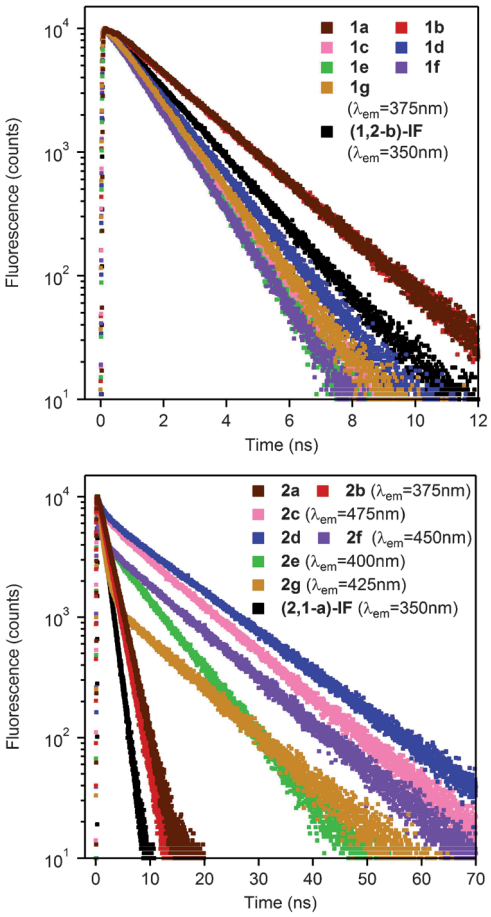

Figure 7. Fluorescence decay curves of **1a–g** and (1,2-*b*)-IF (top) and **2a–g** and (2,1-*a*)-IF (bottom) in solution in THF (λ_{exc} = 330 nm).

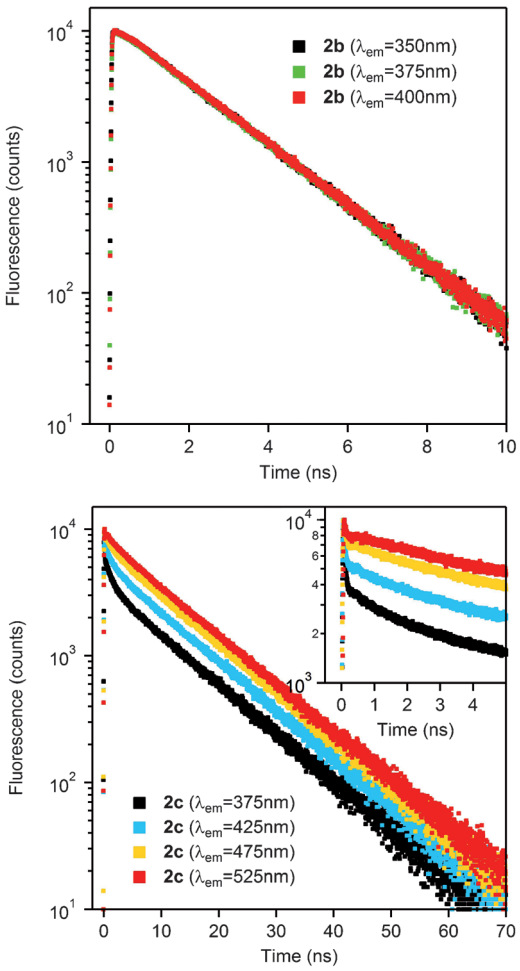

Figure 8. Fluorescence decay curves of **2b** (top) and **2c** (bottom) in solution in THF as a function of emission wavelength (λ_{exc} = 330 nm).

the same range than the lifetimes of **1c–g** (0.90–1.30 ns), and the third one A_3 is very short (<75 ps). This situation is actually a strong indication of the kinetics of excimer formation. In addition, the fluorescence decays of **2c–g** are wavelength-dependent as exemplified in Figure 8, bottom for **2c**. From the full set of decay curves recorded at several emission wavelengths, a general trend can be drawn (see Figure S21): i) for each given compound, the three time-constants were found identical whatever the emission wavelength, ii) the relative contribution of the first time-constant (A_1, slow contribution) increases as the emission wavelength increases, whereas the relative contribution of the third time-constant (A_3, short contribution) decreases as the emission wavelength increases, and iii) the relative contribution of the second time-constant (A_2, intermediate contribution) remains almost constant whatever the emission wavelength. Then, the slower time-constant τ_1, mostly present at higher emission wavelength, is representative of the excimer emission of the "aryl-fluorene-aryl" species. Most of the intensity fraction is actually contained in this slow excimer contribution, as shown by the f_1 values, greater than 0.85 except for **2g** where f_1 is in the range 0.49–0.76. The short time-constant τ_3 represents the deactivation of the "aryl-fluorene-aryl" monomers, forming the intramolecular excimers in a very short time after excitation and leading to a very limited intensity fraction ($f_3<0.04$ in all cases). One can emphasize that no rise time were observed experimentally for **2c–g**. Indeed, at the emission wavelength of the excimers, one could expect a short rise time,[56,57] corresponding to the kinetics of the intramolecular excimer formation process from one excited "aryl-fluorene-aryl" moiety and its neighbor. In the present case, as shown by the very short decay time τ_3 corresponding to the decay of monomers forming excimers, this rise time takes probably place in a few picoseconds or tens of picoseconds at most. Such a rise time would represent a very limited intensity fraction,[56] and may be hidden by the fast decay time τ_3 itself, that is nevertheless almost beyond the time-resolution of our instrument (~10 ps). Indeed, several examples in the literature show that the rise time corresponding to fluorene excimer formation is not always observed.[57,58] The very fast process of intramolecular excimer formation strongly suggests that the "aryl-fluorene-aryl" chromophores in **2c–g** are located closely, in a favorable conformation, and require only a very slight spatial reorganization to form excimers. This close vicinity between the two "aryl-fluorene-aryl" chromophores in the ground state in the **2c–g** series was already highlighted by ^{1}H NMR spectroscopy and electrochemical studies (see above).

The second decay time of **2c–g** ($\tau_2=0.90$–1.30 ns) corresponds quite closely to the lifetimes of the **1c–g** derivatives (1.09–1.34 ns). Its relative contribution to the decay (A_2) stays almost constant over the emission wavelength, but its intensity fraction (f_2) decreases significantly as the emission wavelength increases. Then, it is reasonable to conclude that this intermediate decay represents some very small proportion of emitting monomers which cannot form excimers. It could originate from "aryl-fluorene-aryl" chromophores in a very specific conformation, due to the relative flexibility of the molecules, such that the conformational reorganization to form excimers is too large to take place within the lifetime of the monomer.

Interestingly, derivatives **2c**, **2d**, and **2f** display very similar behaviors: excimer emission wavelength is located between 450 and 457 nm, the slower decay time τ_1 is in a narrow range 11.16–12.99 ns, corresponding to an intensity fraction greater than 0.87. For **2c**, **2d** and **2f**, excimer formation represents the predominant process leading to a well-defined red-shifted emission.

In the case of **2e**, the slower time-constant τ_1 is also predominant ($f_1>0.93$), showing that despite the existence of monomer, most of the emission intensity is due to excimer species. However, the emission wavelength of **2e** is shorter ($\lambda_{em}=413$ nm, see Table 2), and its main time-constant τ_1 is also shorter ($\tau_1=7.56$ ns, see Table 3) than that of its congeners **2c–d** and **2f–g**. In the specific situation of **2e**, the nature of the excimers could be different than for the other derivatives. Indeed, due to the steric hindrance of the *t*Bu-aryl substituents, the π-stacking mode between the two conjugated "aryl-fluorene-aryl" moieties would be less efficient, leading to a less-stabilized excimer geometry. Such a schematic interpretation would explain that the excimer emission is less red-shifted, compared to **2c–d** and **2f–g** (see Section on Theoretical modeling below).

Compared to **2c–f** derivatives, **2g** shows a unique excimer feature (Table 3, Figure 7, bottom). Its slower decay time τ_1 (10.75 ns) is in the same range than **2c–d** and **2f**, but its relative contribution is drastically reduced ($A_1=0.05$–0.17). This observation applies also for the shorter time-constant τ_3, for which $A_3<0.37$, whereas its relative contribution is noticeably larger than 0.37 in all other derivatives **2c–f**. This tendency is accompanied by a stronger contribution of the intermediate time-constant τ_2 ($A_2>0.58$, $f_2=0.24$–0.51) compared to **2c–f**. One can easily conclude that the emission of **2g** is composed of two overlapped contributions: the blue part of the emission spectrum arises mainly from monomers that are unable to form excimers (larger contribution of the intermediate time-constant in the decay curves, structured "monomer-like" emission shoulder in the emission spectrum below 410 nm), whereas the red part of the emission spectrum results from the excimer emission (larger contribution of the slower time-constant, structureless "excimer-like" emission in the spectrum at $\lambda>410$ nm). Then, **2g** represents a borderline situation where both monomers (that cannot form excimers) and excimers can emit. The two bulky *t*Bu substituents borne by the phenyl rings of **2g** are surely responsible for this effect. Indeed, the steric hindrance is quite large, inhibits the spatial approach between two neighboring "aryl-fluorene-aryl" moieties, and allows monomer emission to occur. Nevertheless, due to large degrees of freedom of this "aryl-fluorene-aryl" molecular structure, some very specific conformations may probably lead to excimer formation.

Geometry optimization of **2d** and **2e** in the first singlet excited state indicates a relevant conformational change

from the ground state, Figure 9, akin to that published recently for the non-substituted DSF-IF **2a**.[31] Indeed, the indenofluorene core moves to planarity and the face-to-face fluorene moieties switch from a staggered arrangement in the ground state to an eclipsed conformation in the first singlet excited state. This had no dramatic consequences on the emissive properties of **2a**[31] in contrast to the peculiar properties of phenyl substituted **2c–g** discussed herein. We note that the two pairs of face-to-face phenyl groups align in an open fashion giving the structure of the whole optimized structures a "dragonfly" aspect. We tentatively assign the spectacular excimer emission properties of the **2c–g** series to this close proximity of the aryl-fluorene-aryl groups in the excited state, as previously observed with different systems for instance those based on stilbenophane.[11] Looking closer into the distances between these eclipsed groups in **2d** and **2e**, we find an interesting trend related to the relative bulkiness of the substituent borne by the phenyl groups. As illustrative examples, the calculated distance between the face-to-face apical carbon atoms of the fluorene group in the relaxed geometry in the first singlet excited state is 3.745 Å for **2d** and 3.802 Å for **2e** (this distance was 3.675 Å in **2a**),[31] while the distance between the closest carbon atoms of the face-to-face phenyl group is 3.503 Å for **2d** and 3.664 Å for **2e**. Hence as the bulkiness of the phenyl group substituent increases (as in **2e**) the overlap of the eclipsed face-to-face aryl-fluorene-aryl groups is somehow frustrated which may explain the decrease of the emission wavelength in **2e** compared with **2d**. Similar geometry optimization in the first singlet excited state in the case of **2g** yielded a staggered geometry similar to that of the ground state. This might be explained by the difficulty to converge to an eclipsed conformation with such a large steric hindrance. It is also consistent with the different emissive contributions experimentally found in **2g** (see above).

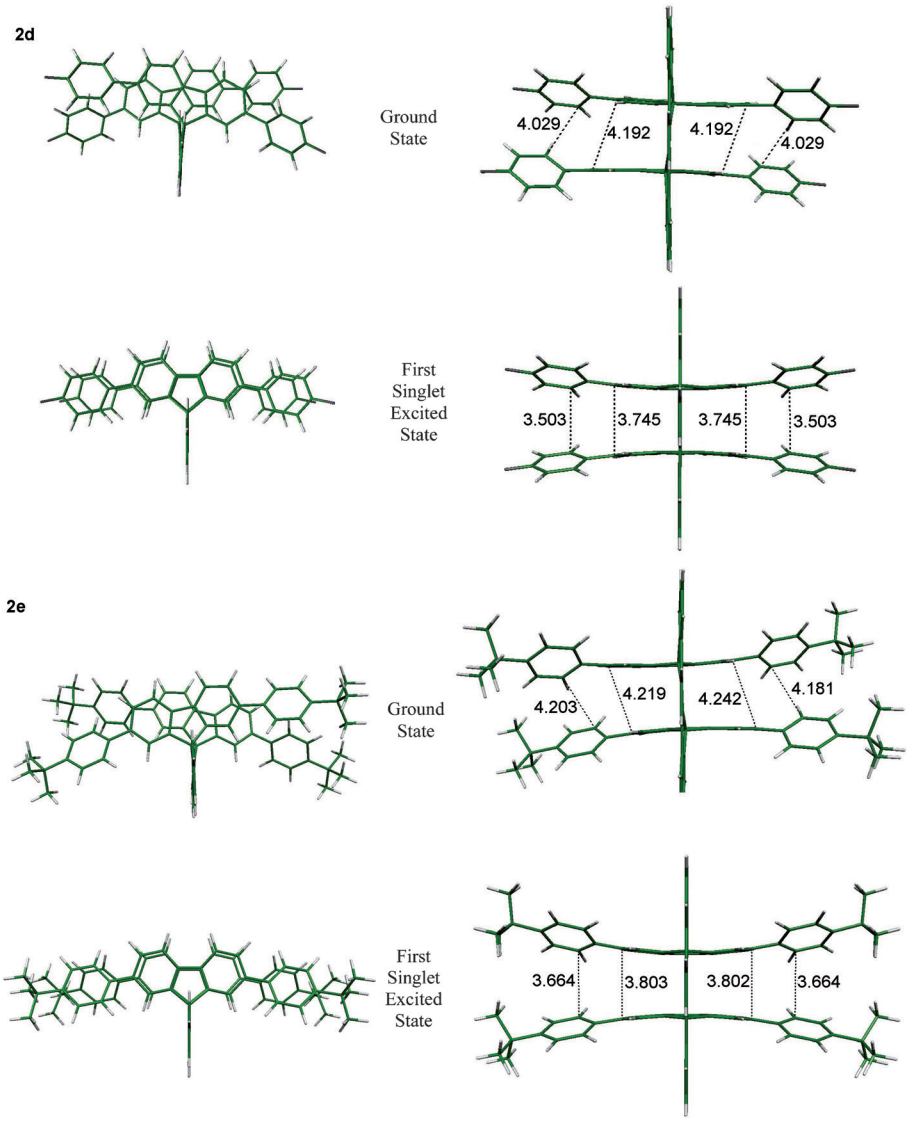

Figure 9. Views of the optimized geometry of **2d** (top) and **2e** (bottom) in their ground state and first singlet excited state with selected relevant distances as discussed in the text.

Conclusion

In summary, we have designed and synthesized via a common intermediate, two families of aryl-substituted DSF-IFs **1c–g** and **2c–g**. Their properties have been studied in detail by a combined experimental and theoretical approach and compared to relevant model compounds (SBF, **m1**) and to their constituting building blocks **1a**/**2a** and (1,2-*b*)-IF/(2,1-*a*)-IF. Due to their different geometries, the two families of aryl-substituted **1c–g** and **2c–g** present drastically different properties. Indeed, the geometry of aryl-substituted **2c–g**, with face-to-face "aryl-fluorene-aryl" moieties, leads to intramolecular π–π interactions in the ground and excited state. The π–π interactions in the ground state between face-to-face "aryl-fluorene-aryl" moieties have been evidenced through detailed ^{1}H NMR, electrochemical and photophysical investigations. Of particular interest was the be-

havior of aryl-substituted **1c–g** and **2c–g** in the excited state. Both **1c–g** and **2c–g** are violet/blue fluorescent emitters with emission wavelengths ranging from about 360 to 460 nm and quantum yields ranging from about 30 to 80%. The aryl-substituted **1c–g** present the properties of both the "aryl-fluorene-aryl" and indenofluorenyl fluorophores. For **2c–g**, the face-to-face arrangement of the "aryl-fluorene-aryl" moieties predominantly leads to intramolecular excimer emission as evidenced by a detailed analysis of fluorescence spectra and decay curves. In addition, aryl-substituted **2c–g** also possess remarkable tunable optical properties. Indeed, the emission color can be easily modulated through the steric hindrance between the adjacent substituted phenyl rings leading to conformationally-controllable intramolecular excimer formation. This strategy constitutes an appealing approach to control and finely tune the fluorescence properties of violet/blue indenofluorene emitters.

Acknowledgements

D.T. thanks the Région Bretagne for a studentship. We wish to thank Dr. N. Audebrand for TGA analyses (Rennes), the CDIFX (Centre de Diffractométrie X-Rennes) for data collections, the C.R.M.P.O (Centre Régional de Mesures Physique de l'Ouest) for mass measurements, the Service de Microanalyse-CNRS (Gif sur Yvette) for CHN analyses, the CINES (Montpellier) for computing time, P. Guillaume, A. de Lardemelle, S. Bivaud for their contributions in the syntheses of 2,7-diaryl-fluorenones and S. Fryars for technical assistance.

[1] *Chem. Mater.* **2011**, *23*, 309–922; Thematic issue: π-Functional Materials (Eds.: J. L. Bredas, S. R. Marder, E. Reichmanis).
[2] *Chem. Rev.* **2007**, *107*, 922-1386; Thematic issue: Organic Electronics and Optoelectronics (Eds.: S. R. Forrest, M. E. Thompson).
[3] A. C. Grimsdale, K. L. Chan, R. E. Martin, P. G. Jokisz, A. B. Holmes, *Chem. Rev.* **2009**, *109*, 897–1091.
[4] T. P. I. Saragi, T. Spehr, A. Siebert, T. Fuhrmann-Lieker, J. Salbeck, *Chem. Rev.* **2007**, *107*, 1011–1065.
[5] A. C. Grimsdale, K. Müllen, *Macromol. Rapid Commun.* **2007**, *28*, 1676–1702.
[6] F. M. Winnik, *Chem. Rev.* **1993**, *93*, 587–614.
[7] B. S. Nehls, F. Galbrecht, A. Bilge, D. J. Brauer, C. W. Lehmann, U. Scherf, T. Farrell, *Org. Biomol. Chem.* **2005**, *3*, 3213–3219.
[8] R. Nandy, S. Sankararaman, *Org. Biomol. Chem.* **2010**, *8*, 2260–2266.
[9] T. Nakano, T. Yade, *J. Am. Chem. Soc.* **2003**, *125*, 15474–15484.
[10] H. Benten, H. Ohkita, S. Ito, M. Yamamoto, N. Sakumoto, K. Hori, Y. Tohda, K. Tani, Y. Nakamura, J. Nishimura, *J. Phys. Chem. B* **2005**, *109*, 19681–19687.
[11] J. Gierschner, H.-G. Mack, D. Oelkrug, I. Waldner, H. Rau, *J. Phys. Chem. A* **2004**, *108*, 257–263.
[12] D. Mansell, N. Rattray, L. L. Etchells, C. H. Schwalbe, A. J. Blake, E. V. Bichenkova, R. A. Bryce, C. J. Barker, A. Diaz, C. Kremer, S. Freeman, *Chem. Commun.* **2008**, 5161–5163.
[13] F. D. Lewis, T. L. Kurth, *Can. J. Chem.* **2003**, *81*, 770–776.
[14] H. S. Jung, M. Park, D. Y. Han, E. Kim, C. Lee, S. Ham, J. S. Kim, *Org. Lett.* **2009**, *11*, 3378–3381.
[15] D. Cornelis, E. Franz, I. Asselberghs, K. Clays, T. Verbiest, G. Koeckelberghs, *J. Am. Chem. Soc.* **2011**, *133*, 1317–1327.
[16] K. M. Knoblock, C. J. Silvestri, D. M. Collard, *J. Am. Chem. Soc.* **2006**, *128*, 13680–13681.
[17] T. Kaikawa, K. Takimiya, Y. Aso, T. Otsubo, *Org. Lett.* **2000**, *2*, 4197–4199.
[18] W. Mróz, J. P. Bombenger, C. Botta, A. O. Biroli, M. Pizzoti, F. De Angelis, L. Belpassi, R. Tubino, F. Meinardi, *Chem. Eur. J.* **2009**, *15*, 12791–12798.
[19] *Organic Light-Emitting Devices: Synthesis, Properties, and Applications* (Eds.: K. Müllen, U. Scherf), Wiley-VCH, Weinheim, **2006**.
[20] J. Salbeck, M. Schörner, P. Fuhrmann, *Thin Solid Films* **2002**, *417*, 20–25.
[21] D. Schneider, T. Rabe, T. Riedl, T. Dobbertin, M. Kröger, E. Becker, H.-H. Johannes, W. Kowalsky, T. Weimann, J. Wang, P. Hinze, A. Gerhard, P. Stössel, H. Vestweber, *Adv. Mater.* **2005**, *17*, 31–34.
[22] N. Johansson, J. Salbeck, J. Bauer, F. Weissörtel, P. Bröms, A. Andersson, W. R. Salaneck, *Adv. Mater.* **1998**, *10*, 1137–1141.
[23] T. Spehr, R. Pudzich, P. Fuhrmann, J. Salbeck, *Org. Electron.* **2003**, *4*, 61–69.
[24] D. Thirion, C. Poriel, F. Barrière, R. Métivier, J. Rault-Berthelot, *Org. Lett.* **2009**, *11*, 4794–4797.
[25] C. Poriel, J. Rault-Berthelot, F. Barrière, A. M. Z. Slawin, *Org. Lett.* **2008**, *10*, 373–376.
[26] C. Poriel, J.-J. Liang, J. Rault-Berthelot, F. Barrière, N. Cocherel, A. M. Z. Slawin, D. Horhant, M. Virboul, G. Alcaraz, N. Audebrand, L. Vignau, N. Huby, L. Hirsch, G. Wantz, *Chem. Eur. J.* **2007**, *13*, 10055–10069.
[27] J. P. Amara, T. M. Swager, *Macromolecules* **2006**, *39*, 5753–5759.
[28] F. Dewhurst, P. K. J. Shah, *J. Chem. Soc. C* **1969**, 1503–1504.
[29] N. Miyaura, A. Suzuki, *Chem. Rev.* **1995**, *95*, 2457–2483.
[30] C. Poriel, F. Barrière, D. Thirion, J. Rault-Berthelot, *Chem. Eur. J.* **2009**, *15*, 13304–13307.
[31] D. Thirion, C. Poriel, J. Rault-Berthelot, F. Barrière, O. Jeannin, *Chem. Eur. J.* **2010**, *16*, 13646–13658.
[32] X. Mei, C. Wolf, *J. Org. Chem.* **2005**, *70*, 2299–2305.
[33] Y. Ting, Y.-H. Lai, *J. Am. Chem. Soc.* **2004**, *126*, 909–914.
[34] R. Rathore, S. H. Abdelwahed, I. A. Guzei, *J. Am. Chem. Soc.* **2003**, *125*, 8712–8713.
[35] W.-L. Wang, J. Xu, Z. Sun, X. Zhang, Y. Lu, Y.-H. Lai, *Macromolecules* **2006**, *39*, 7277–7285.
[36] R. Nandy, M. Subramoni, B. Varghese, S. Sankararaman, *J. Org. Chem.* **2007**, *72*, 938–944.
[37] A. P. Kulkarni, C. J. Tonzola, A. Babel, S. A. Jenekhe, *Chem. Mater.* **2004**, *16*, 4556–4573.
[38] Y.-L. Liao, C.-Y. Lin, Y.-H. Liu, K.-T. Wong, W.-Y. Hung, W.-J. Chen, *Chem. Commun.* **2007**, 1831–1833.
[39] J. Londenberg, T. P. I. Saragi, I. Suske, J. Salbeck, *Adv. Mater.* **2007**, *19*, 4049–4053.
[40] V. J. Chebny, R. Shukla, S. V. Lindeman, R. Rathore, *Org. Lett.* **2009**, *11*, 1939–1942.
[41] N. Cocherel, C. Poriel, J. Rault-Berthelot, F. Barrière, N. Audebrand, A. M. Z. Slawin, L. Vignau, *Chem. Eur. J.* **2008**, *14*, 11328–11342.
[42] S. Merlet, M. Birau, Z. Y. Wang, *Org. Lett.* **2002**, *4*, 2157–2159.
[43] J. Salbeck, N. Yu, J. Bauer, F. Weissörtel, H. Bestgen, *Synth. Met.* **1997**, *91*, 209–215.
[44] J. Salbeck, F. Weissörtel, J. Bauer, *Macromol. Symp.* **1998**, *125*, 121–132.
[45] Covion organic semiconductors: Covion, EP 1491568, **2004**.
[46] R. V. Person, B. R. Peterson, D. A. Lightner, *J. Am. Chem. Soc.* **1994**, *116*, 42–59.
[47] F. D. Lewis, T. L. Kurth, W. Liu, *Photochem. Photobiol. Sci.* **2002**, *1*, 30–37.
[48] M. Kasha, H. R. Rawls, M. Ashraf El-Bayoumi, *Pure Appl. Chem.* **1965**, *11*, 371–392.
[49] G. Heimel, M. Daghofer, J. Gierschner, E. J. W. List, A. C. Grimsdale, K. Müllen, D. Beljonne, J. L. Brédas, E. Zojer, *J. Chem. Phys.* **2005**, *122*, 054501–054511.
[50] M. Belletête, M. Ranger, S. Beaupré, M. Leclerc, G. Durocher, *Chem. Phys. Lett.* **2000**, *316*, 101–107.
[51] T. Fuhrmann, J. Salbeck, *Adv. Photochem.* **2002**, *27*, 83–166.

[52] T. Qin, G. Zhou, H. Scheiber, R. E. Bauer, M. Baumgarten, C. E. Anson, E. J. W. List, K. Müllen, *Angew. Chem.* **2008**, *120*, 8416–8420; *Angew. Chem. Int. Ed.* **2008**, *47*, 8292–8296.
[53] K. R. J. Thomas, J. T. Lin, C.-M. Tsai, H.-C. Lin, *Tetrahedron* **2006**, *62*, 3517–3522.
[54] D. L. Horrocks, W. G. Brown, *Chem. Phys. Lett.* **1970**, *5*, 117–119.
[55] J. L. Scott, T. Yamada, K. Tanaka, *Bull. Chem. Soc. Jpn.* **2004**, *77*, 1697–1701.
[56] B. H. Boo, D. Kang, *J. Phys. Chem. A* **2005**, *109*, 4280–4284.
[57] Y. B. Chung, D.-J. Jang, D. Kim, M. Lee, H. S. Kim, B. H. Boo, *Chem. Phys. Lett.* **1991**, *176*, 453–458.
[58] M. Itoh, Y. Morita, *J. Phys. Chem.* **1988**, *92*, 5693–5696.

Received: March 29, 2011
Published online: August 8, 2011

